

See discussions, stats, and author profiles for this publication at: <https://www.researchgate.net/publication/26678328>

An Alternative Mechanism to Explain the Ruthenium(II)–Catalyzed [2+2+2] Cycloaddition of 1,6–Diyne and Tricarbonyl Compounds

ARTICLE in THE JOURNAL OF PHYSICAL CHEMISTRY A · AUGUST 2009

Impact Factor: 2.69 · DOI: 10.1021/jp900962d · Source: PubMed

READS

26

3 AUTHORS:



M. Merced Montero-Campillo

Universidad Autónoma de Madrid

28 PUBLICATIONS 147 CITATIONS

SEE PROFILE



Jesus Rodriguez-Otero

University of Santiago de Compostela

120 PUBLICATIONS 1,429 CITATIONS

SEE PROFILE



Enrique M Cabaleiro-Lago

University of Santiago de Compostela

98 PUBLICATIONS 1,169 CITATIONS

SEE PROFILE

An Alternative Mechanism to Explain the Ruthenium(II)-Catalyzed [2 + 2 + 2] Cycloaddition of 1,6-Diynes and Tricarbonyl Compounds

M. Merced Montero-Campillo,[†] Jesús Rodríguez-Otero,^{*,†} and Enrique M. Cabaleiro-Lago[‡]

Departamento de Química Física, Facultade de Química, Universidade de Santiago de Compostela, Avda. das Ciencias s/n, 15782 Santiago de Compostela, Galicia, Spain, and Departamento de Química Física, Facultade de Ciencias, Universidade de Santiago de Compostela, Campus de Lugo, Avda. Alfonso X El Sabio s/n 27002 Lugo, Galicia, Spain

Received: February 2, 2009; Revised Manuscript Received: May 4, 2009

Density functional theory has been used to study an alternative mechanism for the ruthenium(II)-catalyzed [2 + 2 + 2] cycloaddition between 1,6-diynes and tricarbonyl compounds, proposing a multistep-pathway different from that which we previously reported. The dimerization mechanism to obtain the minority product of the reaction has also been studied in order to analyze the selectivity of this cycloaddition.

Introduction

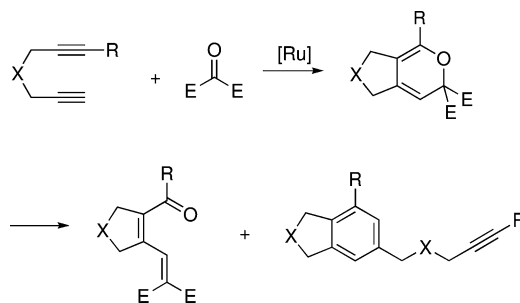
In recent years, transition metal catalyzed multicomponent cycloadditions have contributed extensively to organic synthesis.^{1–3} The use of ruthenium complexes in those reactions is gaining importance due to their demonstrated ability in the catalytic carbon–carbon bond formations via ruthenacycle intermediates.^{4,5}

During our studies of different transition metal catalyzed cycloadditions,⁶ we proposed a comprehensive reaction mechanism for the Ru(II)-catalyzed [2 + 2 + 2] cycloaddition of 1,6-diynes and tricarbonyl compounds.⁷ Previously, this cycloaddition had been experimentally studied by Yamamoto and co-workers (see Scheme 1) and the sketch of its reaction mechanism suggested.⁸ Now in this work we propose a different mechanism based on our previous experience with this type of unsaturated substrates in transition metal cycloadditions.

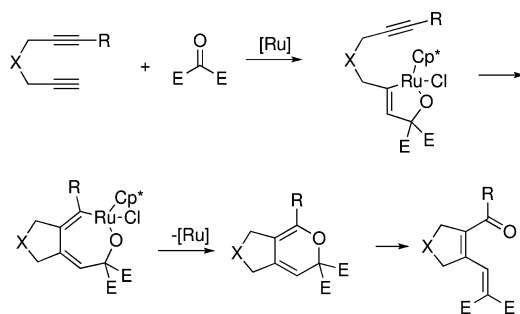
Yamamoto's mechanism begins with an oxidative cyclization between one of the alkynes of the 1,6-diyne and the ketone carbonyl group to produce an oxaruthenacyclopentene intermediate, followed by the insertion of the other alkyne and the reductive elimination of the ruthenium catalyst.⁸ The last step involves an electrocyclic ring opening (see Scheme 2). In our previous study of this [2 + 2 + 2] cycloaddition we reported the structures and energy barriers of this reaction mechanism.⁷ In the present paper we propose that the catalytic cycle could begin with an oxidative coupling between the ruthenium catalyst and the 1,6-diyne, followed by the insertion of the central carbonyl group of the tricarbonyl compound. The reductive elimination and the electrocyclic ring-opening steps are the same as in our previous study (see Scheme 3).

Although the dienone is the main product of the cycloaddition, there is a secondary product due to the dimerization of the 1,6-diyne reactant. Two possible reaction mechanisms have been studied for a better understanding of this dimerization and the whole [2 + 2 + 2]-cycloaddition. So, the goal of this work is to provide a more complete vision of the reaction contributing with new information about the catalytic cycle.

SCHEME 1: Ru(II)-Catalyzed [2 + 2 + 2] Cycloaddition Reported by Yamamoto and Co-workers⁸ (X = O, NTs, C(CO₂Me)₂, C(Ac)₂, C(CH₃)₂; E = CO₂Et; R = alkyl, H)



SCHEME 2: [2 + 2 + 2]-Cycloaddition Mechanism Proposed by Yamamoto and Co-workers (X = O, NTs, C(CO₂Me)₂, C(Ac)₂, C(CH₃)₂; E = CO₂Et; R = alkyl, H)^a



^a A theoretical study of this proposal was previously carried out by the authors of the present work.⁷

Computational Details

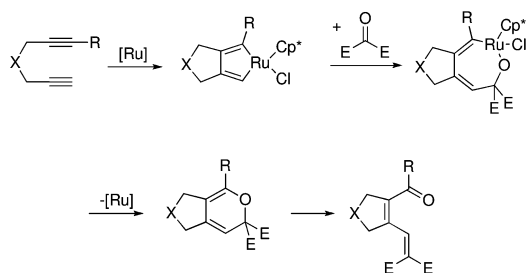
Calculations were carried out with density functional theory (DFT) employing B3LYP functional. B3LYP combines the three-coefficient-dependent hybrid functional for the exchange energy proposed by Becke (B3) with the correlation functional proposed by Lee, Yang, and Parr (LYP).⁹ 6-31G(d) Pople's basis set was used for C, O, H, and Cl atoms, and the effective core potential LANL2DZ was used for the Ru atom.¹⁰ This chosen methodology and basis set are a usual choice in this kind of transition metal reaction calculations.¹¹ All the stationary points were characterized as minima or transition states by the

* Corresponding author, r.otero@usc.es.

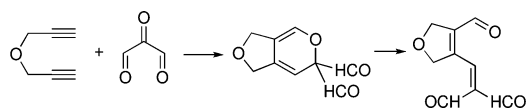
[†] Departamento de Química Física, Facultade de Química, Universidade de Santiago de Compostela, Avda. das Ciencias s/n.

[‡] Departamento de Química Física, Facultade de Ciencias, Universidade de Santiago de Compostela, Campus de Lugo.

SCHEME 3: Proposed Alternative Reaction Mechanism ($X = O, NTs, C(CO_2Me)_2, C(Ac)_2, C(CH_3)_2$; $E = CO_2Et$; $R = \text{alkyl, H}$)



SCHEME 4: $X = O, R = H$, and $E = HCO$ were Chosen in Scheme 1 to Model the [2 + 2 + 2] Cycloaddition



vibrational frequency analysis, using analytical second derivatives. For every reaction, the intrinsic reaction coordinate (IRC) path was traced in order to check the energy profiles connecting each TS to the two associated minima. All calculations were carried out with the Gaussian03 program.¹²

Results and Discussion

In our study, we have simplified the experimental reactants as Scheme 4 shows in order to make a comparison between the previous results and the current ones. The catalyst used in the cycloaddition is the $[Cp^*Ru(cod)Cl]$ complex which active species as catalyst is a complex formed by the ruthenium atom

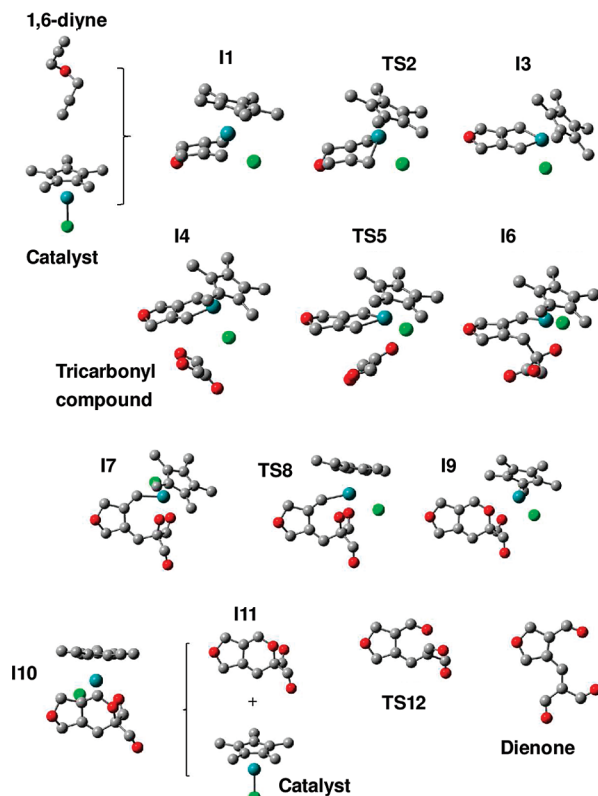
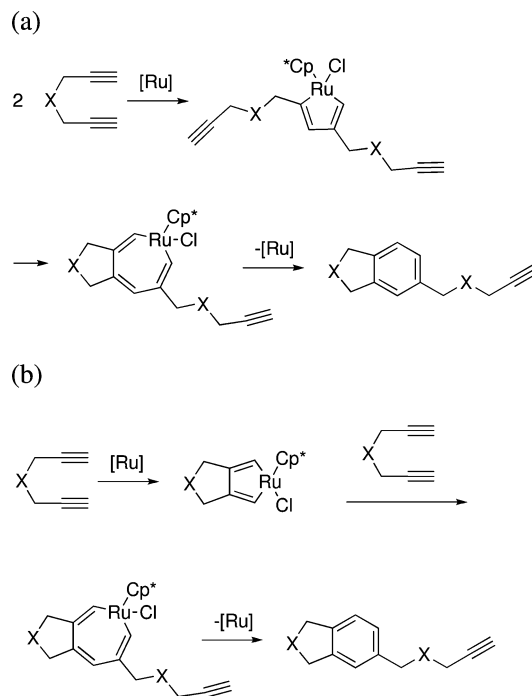


Figure 1. Alternative mechanism: reactant, product, intermediate, and transition state structures at the B3LYP/6-31G(d)+LANL2DZ level.

TABLE 1: Alternative Mechanism: Absolute and Relative Electronic Energies (ZPE included) in Atomic Units and kcal/mol at B3LYP/6-31G(d,p)+LANL2DZ Level

	E_{ZPE} (u.a.)	ΔE_{ZPE} (kcal/mol)
diyne + diformyl ketone + catalyst	-1592.27720	0.00
I1	-1251.23555	
TS2	-1251.22081	
I3	-1251.28228	
I1 + diformyl ketone		-21.46
TS2 + diformyl ketone		-12.21
I3 + diformyl ketone		-50.78
I4	-1592.37119	-58.98
TS5	-1592.35997	-48.62
I6	-1592.38320	-66.52
I7	-1592.39662	-74.94
TS8	-1592.35651	-49.77
I9	-1592.42540	-92.99
I10	-1592.43558	-99.39
I11 + catalyst	-1592.40684	-81.35
TS12 + catalyst	-1592.38252	-66.09
product + catalyst	-1592.42074	-90.08

SCHEME 5: Two Possible Pathways to Obtain the Minority Product of the Reaction ($X = O$)



and the pentamethylcyclopentadienyl (Cp^*) and chlorine ligands.^{13,8} The reactant, intermediate, transition state, and product structures obtained at the B3LYP/6-31G(d)+LANL2DZ level are shown in Figure 1.

I1 is the first structure of the catalytic cycle, a complex formed by the catalyst and the 1,6-diyne in which the transition metal is coordinated to the two reactant triple bonds. The ligands adopt a tetrahedral geometry around the metal. This first step of the cycloaddition involves an oxidative coupling (see transition state **TS2**) where a bicyclic structure is being formed due to the interaction between two of the triple-bonded carbons, **I3** is the resulting intermediate. The next step involves the addition of the carbonyl group of the second reactant, the diformyl ketone. **I3** and the reactant form a complex, **I4**, which through transition state **TS5** reaches the heptametalacyclo **I6**. This first part of the pathway shows important differences with

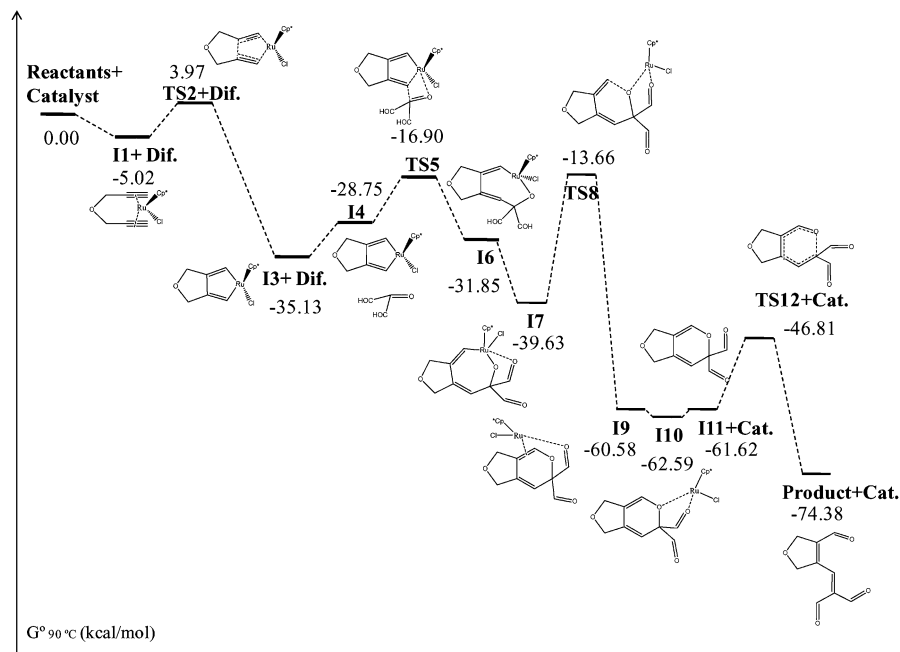


Figure 2. Alternative mechanism: Free energy profile ($T = 90\text{ }^{\circ}\text{C}$) at B3LYP/6-31G(d)+LANL2DZ level (Dif. = diformyl ketone, Cat. = catalyst).

that we previously reported; in that case the oxidative addition took place between the carbonyl group and the alkyne followed by the second alkyne insertion.

The next steps of the pathway are coincident with those described in the first study.⁷ The reductive elimination of the catalyst takes place in the step **I7**–**TS8**–**I9**, while the last step involves an electrocyclic ring-opening, a concerted reaction in which the C–O bond is being broken through a disrotatory movement (**TS12**).¹⁴

The free energy profile of the whole reaction (at $90\text{ }^{\circ}\text{C}$, the experimental temperature of the reaction) is summarized in Figure 2; Table 1 contains the absolute and relative electronic energy values. The TS corresponding to the oxidative coupling in the first step of the catalytic cycle is about 4 kcal/mol relative to the reactants, a value which is very far away from the ~ 28 kcal/mol needed for the coupling between the alkyne and the carbonyl group obtained in our previously reported study based on Yamamoto's proposal.⁷ The second step has a barrier around 18 kcal/mol (**I3** + diformyl ketone to **TS5**). Taking into account that the remaining steps are the same and that the bottleneck of the cycloaddition was that first addition, we can conclude that this alternative mechanism is much more feasible than the previously proposed.⁷

Scheme 5 shows two possible mechanisms to explain the dimerization of the reactant 1,6-diyne, the secondary product of the cycloaddition. The main difference between them is the way in which the coupling takes place: in the first one, the ruthenium catalyst forms a complex with two different molecules of the reactant; in the second one, the two alkynes of one reactant molecule are complexed with the catalyst and then a second reactant molecule is inserted in the metallacycle. Figures 3 and 4 show the two studied pathways. The mechanisms were equivalent to those we described for the main product. In Figure 3, **I1'**–**TS2'**–**I3'** is the oxidative coupling between two different molecules of reactant. The conformer **I4'** presents a more favorable position for the next alkyne insertion (**TS5'**) which is completely inserted in **I6'**. The last step, **I7'**–**TS8'**–**I9'**, is the reductive elimination of the ruthenium catalyst. Figure 4 shows the second option: one molecule of 1,6-diyne forms a

TABLE 2: Dimerization Mechanisms a and b: Absolute and Relative Electronic Energies (ZPE included) in Atomic Units and kcal/mol at the B3LYP/6-31G(d,p)+LANL2DZ Level

dimerization mechanism a	E_{ZPE} (u.a.)	ΔE_{ZPE} (kcal/mol)
catalyst + 2 diyne	–1558.39400	0.00
I1'	–1558.42985	–22.49
TS2'	–1558.40959	–9.78
I3'	–1558.48687	–58.28
I4'	–1558.47864	–53.11
TS5'	–1558.47626	–51.62
I6'	–1558.51883	–78.33
I7'	–1558.54009	–91.67
TS8'	–1558.53739	–89.98
I9'	–1558.63722	–152.62
dimerization mechanism b	E_{ZPE} (u.a.)	ΔE_{ZPE} (kcal/mol)
catalyst + 2 diyne	–1558.39400	0.00
I1' + diyne	–1558.42820	–21.46
TS2' + diyne	–1558.41346	–12.21
I3' + diyne	–1558.47493	–50.78
I4'	–1558.47545	–51.11
TS5'	–1558.47297	–49.55
I6'	–1558.51184	–73.94
I7'	–1558.54014	–91.67
TS8'	–1558.53349	–87.53
I9'	–1558.63727	–152.65

ruthenacycle (**I1'**–**TS2'**–**I3'**) and then an alkyne of a second molecule is added to this ruthenacycle (**I4'**–**TS5'**–**I6'**); the remaining part of the mechanism is the same as in the first option, a reductive elimination. The two dimerization pathways can be compared in Table 2 and Figure 5, which summarize the absolute and relative electronic energies and the corresponding free energy profile at $90\text{ }^{\circ}\text{C}$. The key step is clearly the first one since the coupling is easier between two triple bonds of the same molecule than from different molecules. So, dimerization pathway b will be preferred to pathway a.

At this point, it is worth noting that the alternative main mechanism (Figures 1 and 2) and the dimerization mechanism

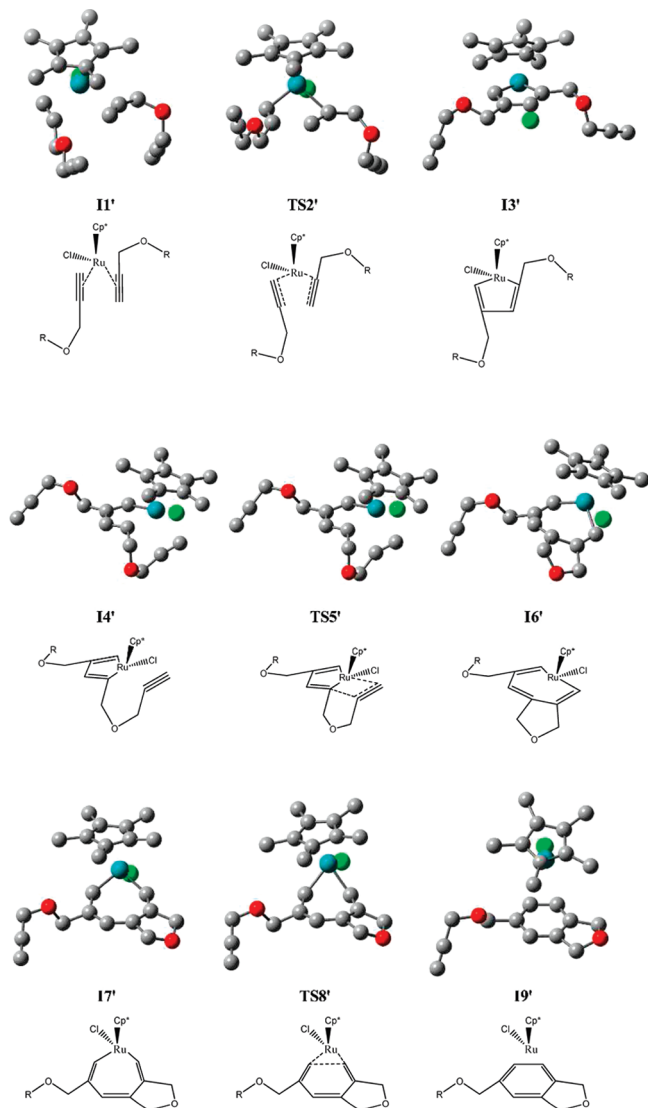


Figure 3. Dimerization mechanism a: reactant, product, intermediate, and transition state structures at the B3LYP/6-31G(d)+LANL2DZ level.

b (Figures 4 and 5) have a common part: the same first step. Then, the next addition of a diformyl ketone molecule or another diyne molecule will lead to the main product or to the diyne dimer, respectively. Setting an appropriate comparison between the two pathways (alternative main path and dimerization (b)), the electronic energy difference is only 0.22 kcal/mol favorable to the main path.¹⁵ This virtually inexistent difference lead us to think that the two mechanisms will be competitive at this calculation level. This is not in contradiction with the experimental results, since there is not enough information about the experimental reaction selectivity in several of the studied cases, and in particular in the most similar to our model reaction (scheme 4). Moreover, changes in the diyne's X group or the use of unsymmetrical diynes could be decisive to discriminate the competitive processes, as commented on in the paper by Yamamoto et al.⁸

Finally, it is important to observe that the comments made in the final part of the previous work (about the general vision of the cotrimerization of alkynes and double bonds) are still valid here. Now, we have just studied a new pathway for the first part of the cycloaddition; even so, the dimerization mechanism also fits properly in those considerations.⁷

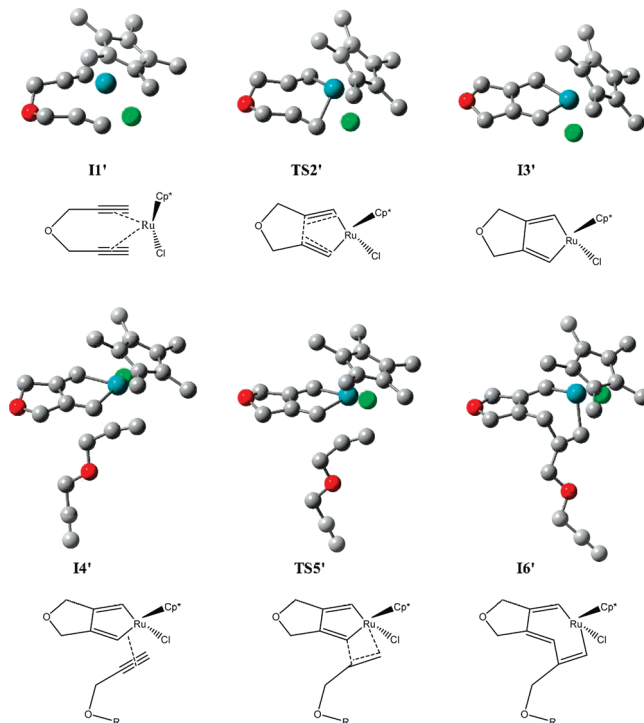


Figure 4. Dimerization mechanism b: reactant, product, intermediate, and transition state structures at the B3LYP/6-31G(d)+LANL2DZ level. The remaining structures (I7'–TS8'–I9') are the same as in mechanism a.

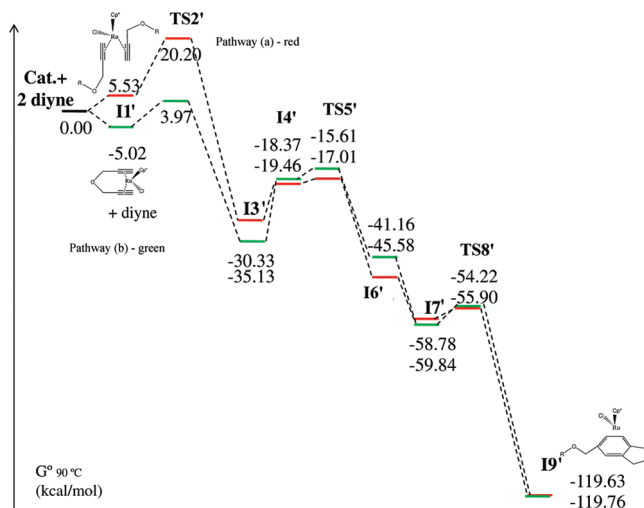


Figure 5. Comparison between dimerization mechanisms a and b: Free energy profile ($T = 90\text{ }^{\circ}\text{C}$) at B3LYP/6-31G(d)+LANL2DZ level (Cat. = catalyst).

Conclusions

The study of the reaction mechanism of the ruthenium-catalyzed [2 + 2 + 2] cycloaddition between 1,6-diynes and tricarbonyl compounds is now more complete due to the exploration of a different pathway. The reaction mechanism was studied using density functional theory comparing this multistep process with the previously reported one.⁷ According to our results, this new proposal has substantially lower activation energies. The selectivity of the reaction was also analyzed and two possible dimerization mechanisms of the secondary product were studied. One of these two potential dimerization processes could be competitive with the alternative main path, at least for the simplified reactants used in our computational study.

Acknowledgment. The authors thank the Xunta de Galicia for financial support “Axuda para a Consolidación e Estructuración de unidades de investigación competitivas do Sistema Universitario de Galicia, 2007/50, cofinanciada polo FEDER 2007-2013”. The authors express their gratitude to the CESGA (Centro de Supercomputación de Galicia), and M.M.M.-C. is grateful for financial support from Xunta de Galicia by the María Barbeito contract.

Supporting Information Available: Cartesian coordinates for structures shown in Figure 1 and absolute and relative free energy (B3LYP/6-31G*+LANL2DZ, 90 °C) for dimerization mechanisms a and b. This material is available free of charge via the Internet at <http://pubs.acs.org>.

References and Notes

- (1) Lautens, M.; Klute, W.; Tam, W. *Chem. Rev.* **1996**, 96, 49.
- (2) Ojima, I.; Tzamarioudaki, M.; Li, Zhaoyang; Donovan, Robert J. *Chem. Rev.* **1996**, 96, 635.
- (3) Crabtree, R. H. *The Organometallic Chemistry of the Transition Metals*, 4th ed.; Wiley: New York, 2005.
- (4) (a) Shiotsuki, M.; Ura, Y.; Ito, T.; Wada, K.; Kondo, T.; Mitsudo, T. *J. Organomet. Chem.* **2004**, 689, 3168. (b) Varela, J. A.; González-Rodríguez, C.; Rubín, S. G.; Castedo, L.; Saá, Carlos. *J. Am. Chem. Soc.* **2006**, 128, 9576. (c) Varela, J. A.; Rubín, S. G.; González-Rodríguez, C.; Castedo, L.; Saá, C. *J. Am. Chem. Soc.* **2006**, 128, 9262. (d) Casey, C. P.; Clark, T. B.; Guzei, I. A. *J. Am. Chem. Soc.* **2007**, 129, 11821.
- (5) (a) Naota, T.; Takaya, H.; Murahashi, S. I. *Chem. Rev.* **1998**, 98, 2599. (b) Trost, B. M.; Toste, F. D.; Pinkerton, A. B. *Chem. Rev.* **2001**, 101, 2067. (c) *Ruthenium in Organic Synthesis*; Murahashi, S. I., Ed.; Wiley-VCH: Weinheim, 2004. (d) *Ruthenium Catalysts and Fine Chemicals*; Bruneau, C., Dixneuf, P. H., Eds.; Springer: New York, 2004.
- (6) (a) Montero-Campillo, M. M.; Rodríguez-Otero, J.; Cabaleiro-Lago, E. M. *J. Phys. Chem. A* **2008**, 112, 2423. (b) Montero-Campillo, M. M.; Rodríguez-Otero, J.; Cabaleiro-Lago, E. M. *Tetrahedron* **2008**, 64, 6215.
- (c) Montero-Campillo, M. M.; Cabaleiro-Lago, E. M.; Rodríguez-Otero, J. *J. Phys. Chem. A* **2008**, 112, 9068.
- (7) Rodríguez-Otero, J.; Montero-Campillo, M. M.; Cabaleiro-Lago, E. M. *J. Phys. Chem. A* **2008**, 112, 8116.
- (8) Yamamoto, Y.; Takagishi, H.; Itoh, K. *J. Am. Chem. Soc.* **2002**, 124, 6844–6845.
- (9) (a) Lee, C.; Yang, W.; Parr, R. J. *Phys. Rev. B* **1988**, 37, 785. (b) Becke, A. D. *J. Chem. Phys.* **1993**, 98, 5648.
- (10) Hay, P. J.; Wadt, W. R. *J. Chem. Phys.* **1985**, 82, 299.
- (11) See for example: (a) Yu, Zhi-Xiang; Wender, P. A.; Houk, K. N. *J. Am. Chem. Soc.* **2004**, 126, 9154. (b) Cadierno, V.; García-Garrido, S. E.; Gimeno, J.; Varela-Álvarez, A.; Sordo, J. A. *J. Am. Chem. Soc.* **2006**, 128, 1360. (c) Böhme, U. *J. Organomet. Chem.* **2006**, 691, 4400.
- (12) Frisch, M. J.; Trucks, G. W.; Schlegel, H. B.; Scuseria, G. E.; Robb, M. A.; Cheeseman, J. R.; Montgomery, J. A., Jr.; Vreven, T.; Kudin, K. N.; Burant, J. C.; Millam, J. M.; Iyengar, S. S.; Tomasi, J.; Barone, V.; Mennucci, B.; Cossi, M.; Scalmani, G.; Rega, N.; Petersson, G. A.; Nakatsuji, H.; Hada, M.; Ehara, M.; Toyota, K.; Fukuda, R.; Hasegawa, J.; Ishida, M.; Nakajima, T.; Honda, Y.; Kitao, O.; Nakai, H.; Klene, M.; Li, X.; Knox, J. E.; Hratchian, H. P.; Cross, J. B.; Adamo, C.; Jaramillo, J.; Gomperts, R.; Stratmann, R. E.; Yazyev, O.; Austin, A. J.; Cammi, R.; Pomelli, C.; Ochterski, J. W.; Ayala, P. Y.; Morokuma, K.; Voth, G. A.; Salvador, P.; Dannenberg, J. J.; Zakrzewski, V. G.; Dapprich, S.; Daniels, A. D.; Strain, M. C.; Farkas, O.; Malick, D. K.; Rabuck, A. D.; Raghavachari, K.; Foresman, J. B.; Ortiz, J. V.; Cui, Q.; Baboul, A. G.; Clifford, S.; Cioslowski, J.; Stefanov, B. B.; Liu, G.; Liashenko, A.; Piskorz, P.; Komaromi, I.; Martin, R. L.; Fox, D. J.; Keith, T.; Al-Laham, M. A.; Peng, C. Y.; Nanayakkara, A.; Challacombe, M.; Gill, P. M. W.; Johnson, B.; Chen, W.; Wong, M. W.; Gonzalez, C.; Pople, J. A. *Gaussian 03, Revision C.01*; Gaussian, Inc: Wallingford, CT, 2004.
- (13) Oshima, N.; Suzuki, H.; Moro-Oka, Y. *Chem. Lett.* **1984**, 1161.
- (14) Woodward, R. B.; Hoffmann, R. *The Conservation of Orbital Symmetry*; Verlag Chemie: Weinheim, 1970.
- (15) Energy (TS5' + diformyl ketone) = −1899.54881 a.u. (dimerization mechanism (b)); energy (TS8 + diyne) = −1899.54916 a.u. (alternative main mechanism); $\Delta E = 0.22$ kcal/mol. The crucial points of the two pathways are almost coincident.

JP900962D